www.ietdl.org

Published in IET Power Electronics
Received on 12th March 2011
Revised on 29th June 2011
doi: 10.1049/iet-pel.2011.0098

ISSN 1755-4535

Family of non-isolated zero current transition bi-directional converters with one auxiliary switch

M. Ahmadi M.R. Mohammadi E. Adib H. Farzanehfard

Department of Electrical and Computer Engineering, Isfahan University of Technology, Isfahan, Iran
E-mail: ahmadi.iut@gmail.com

Abstract: A new family of non-isolated zero current transition bi-directional converters is introduced. Basic non-isolated bi-directional DC–DC converters are derived by combining basic DC–DC converters and they are able to transfer energy between two DC sources using two main switches. In the proposed bi-directional converters, instead of using two independent auxiliary circuits for each main switch, same components with a single auxiliary switch is used to provide soft commutation at both modes of converter operation. In addition, the soft switching range in the proposed converters is not dependent on the duty cycle and the auxiliary circuit is applied only once in each switching cycle, which leads to a simple control circuit. Low weight, small volume, high efficiency and the ease of control are the most important benefits of the proposed converters. The proposed bi-directional buck and boost converter is fully analysed for both buck and boost operating modes. The validity of theoretical analysis is justified using experimental results of a 200 W, 50–100 V prototype converter.

1 Introduction

In recent years, using bi-directional DC–DC converters (BDCs) in different applications is being developed. BDCs are able to transfer energy between two DC sources, in either direction. As BDCs are capable of reversing the direction of current flow, these converters are increasingly applied in applications like hybrid electric/fuel cell vehicles [1–5], DC uninterruptible power supplies [6, 7], fuel cell and battery equalisation [8–11] and photovoltaic applications [12, 13].

Various BDCs can be divided into the non-isolated BDCs and isolated BDCs. The isolated type is required when the converter input and output sides cannot be grounded simultaneously or high voltage gain is required. In this case, a transformer is required which contributes to extra cost and losses. Thus, when high voltage ratio is not needed, non-isolated BDCs are always employed for their simple structure and control scheme. Four basic non-isolated BDCs are derived by combining basic converters (buck, boost, buck–boost, Cuk, SEPIC and Zeta). The resulting converters are buck and boost, buck–boost/buck–boost, SEPIC/Zeta and Cuk/Cuk.

To reduce the volume of switching converters and increase the power density, high switching frequency is required. However, in hard switching converters, when the frequency increases, switching losses and electromagnetic interference increase. To solve these problems, soft switching converters are employed.

In comparison to unidirectional converters, it is more challenging to develop soft switching for BDCs owing to more switches and complex energy flow. Zero voltage transition (ZVT) and zero current transition (ZCT) are two techniques which incorporate soft switching function into conventional pulse width modulation (PWM) converters using auxiliary circuits [14–27]. Some of these auxiliary circuits are employed for the non-isolated BDCs to obtain soft commutation [28–36]. To avoid complexity in ZVT and ZCT BDCs, it is desirable to share auxiliary elements to provide soft switching in both power flow directions. In [28–31], the idea of auxiliary circuits introduced previously in [16, 17] are employed and then the number of auxiliary components are reduced (one inductor, two auxiliary switches and a snubber capacitor). However, in [28, 29], the auxiliary switches turns off under hard switching condition. In [30], soft switching condition is lost at operating duty cycles lower than 0.5. In [31], the main switches and the auxiliary switch are switched in every switching cycle, which results in higher switching losses and complexity of the control circuit. Another non-isolated ZVT BDC is proposed in [32], which uses the previously proposed auxiliary circuit in [17]. In [32], all switches are soft switched and the duty cycle is not limited. However, two split input voltages are required by means of inserting two equal capacitors between the input line and ground. Besides, in order to balance the capacitors, the auxiliary circuit is applied two times in a switching cycle resulting in a more complex control circuit and increased switching losses. In [33], a combination of ZVT buck [16] and ZVT boost [18] converters is used. But this converter suffers from high number of circuit elements. Also, in [34] a combination of ZVT boost [17] and ZCT buck [24], and in [35] a combination of ZCT boost [14] and ZCT buck [14] are used with same resonant elements. In [34–36], the

number of auxiliary elements is reduced but still two auxiliary switches are required.

In this paper, a new family of non-isolated ZCT BDC is introduced. In contrast to previously introduced non-isolated ZVT and ZCT BDCs, the proposed converter uses only one auxiliary switch which provides considerable reduction in cost, volume and weight. The auxiliary components create a simple auxiliary circuit that is based on well-known ZCT technique and is developed based on the fact that LC resonance can create a bidirectional current. The role of the auxiliary switch is to start the required resonance and provide the required path for resonant current. In fact, instead of using two independent auxiliary circuits for each main switch, same components with a single auxiliary switch is used to provide bidirectional current path to obtain soft commutation at both modes of BDC operation. Besides, the soft switching range in the proposed converters is not dependent on duty cycle (in contrast to [30]) and the auxiliary circuit is applied only once in a switching cycle (in contrast to [31]), which leads to a simple control circuit. To verify the operation of the proposed converters, operating modes and design considerations of a buck and boost converter are presented. Finally, the 200 W prototype of the proposed converter is implemented to confirm the theoretical analysis.

2 Circuit description and operation

The proposed converter shown in Fig. 1 is composed of two main switches, S_1 and S_2, one auxiliary switch, S_a, two resonant inductors, L_{S1} and L_{S2}, a resonant capacitor, C_r, and main inductor, L. The converter has nine different operating intervals in a switching cycle in both buck and boost modes. To simplify the converter analysis, it is assumed that inductor L is large enough to be considered as a current source in a switching cycle. Also, the output voltage is assumed constant and modelled by a voltage source. Besides, it is assumed that all elements are ideal, and the converter is operating in steady-state condition. Detailed theoretical analysis for both buck and boost modes are presented below.

2.1 Boost mode of operation

In this mode, S_1 and S_a are the main and auxiliary switches, respectively. The proposed converter has nine operating intervals in this mode as shown in Fig. 2, where the arrows refer to the actual direction of currents and the voltage polarity of C_r refer to voltage polarity at the beginning of each interval. The key waveforms of the converter in this mode are illustrated in Fig. 3 according to the direction of currents and the polarity of the resonant capacitor, C_r, defined in Fig. 1. Before the first interval, it is assumed that all switches are off and the input current is transferred to the V_2 through the body diode of S_2, and C_r voltage is $-V_{C0}$. Besides, it is assumed that $L_{S1} = L_{S2} = L_S$.

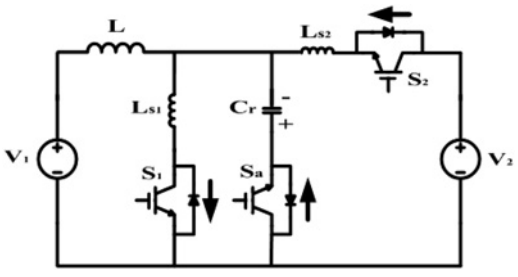

Fig. 1 *Proposed ZCT bidirectional buck-and-boost converter*

Interval 1: $[t_0 - t_1]$ (Fig. 2*a*): At t_0, the main switch S_1 is turned on under zero current switching (ZCS) condition because of inductors L_{S1} and L_{S2}. According to (1), S_1 current increases linearly to input current I_{in} and prepares the condition for the body diode of S_2 to turn off under ZCS condition.

$$I_{S1} = \frac{V_2}{2L_S}(t - t_0) \tag{1}$$

At the end of this interval, S_1 current reaches I_{in}, and the body diode of S_2 turns off under ZCS condition.

Interval 2: $[t_1 - t_2]$ (Fig. 2*b*): During this interval, I_{in} flows through S_1. This operating interval is identical to the switch-on stage of any PWM boost converter.

Interval 3: $[t_2 - t_3]$ (Fig. 2*c*): By turning S_a on under ZCS condition at the beginning of this interval, L_{S1}, L_{S2} and C_r form a resonance through S_1, S_a, and the body diode of S_2. The body diode of S_2 turns on under ZCS condition. S_1 and S_2 currents and C_r voltage equations are as follows

$$I_{S1} = I_{in} + \frac{V_2}{2L_S}(t - t_2) + \left(\frac{2V_{C0} - V_2}{4Z_0}\right)\sin(\omega_0(t - t_2)) \tag{2}$$

$$I_{S2} = \frac{V_2}{2L_S}(t - t_2) - \left(\frac{2V_{C0} - V_2}{4Z_0}\right)\sin(\omega_0(t - t_2)) \tag{3}$$

$$V_{C_r} = -\left(\frac{V_2}{2} + \left(V_{C0} - \frac{V_2}{2}\right)\cos(\omega_0(t - t_2))\right) \tag{4}$$

where

$$\omega_0 = \sqrt{\frac{1}{LC_r}}, \quad Z_0 = \sqrt{\frac{L}{C_r}} \tag{5}$$

$$L = L_{S1}||L_{S2} = L_S/2$$

This interval ends when I_{S2} current reaches zero, and C_r charges to V_{C1}. At the end of this interval, S_1 current is equal to I_1.

Interval 4: $[t_3 - t_4]$ (Fig. 2*d*): In this interval, L_{S1} and C_r continue to resonate through S_1 and S_a. During this interval, S_1 current and C_r voltage are

$$I_{S1} = I_{in} - (I_{in} - I_1)\cos(\omega_1(t - t_3)) + \frac{V_{C1}}{Z_1}\sin(\omega_1(t - t_3)) \tag{6}$$

$$V_{C_r} = -(Z_1(I_{in} - I_1)\sin(\omega_1(t - t_3)) + V_{C1}\cos(\omega_1(t - t_3))) \tag{7}$$

where

$$\omega_1 = \sqrt{\frac{1}{L_S C_r}}, \quad Z_1 = \sqrt{\frac{L_S}{C_r}} \tag{8}$$

This interval ends when S_a current becomes zero, and S_1 current decreases from I_1 to I_{in}. It is assumed that C_r is charged to V_{C2} at the end of this interval.

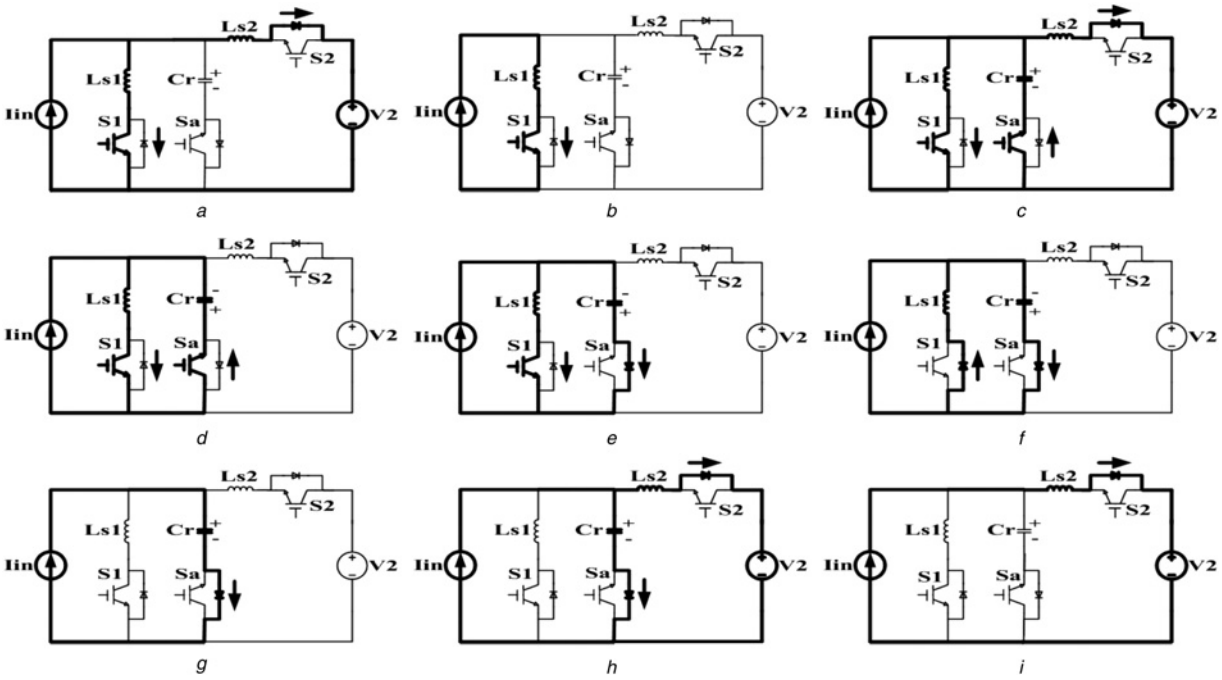

Fig. 2 *Equivalent circuit for each operating interval of the proposed converter in boost mode*

a $[t_0 - t_1]$
b $[t_1 - t_2]$
c $[t_2 - t_3]$
d $[t_3 - t_4]$
e $[t_4 - t_5]$
f $[t_5 - t_6]$
g $[t_6 - t_7]$
h $[t_7 - t_8]$
i $[t_8 - t_0 + T]$

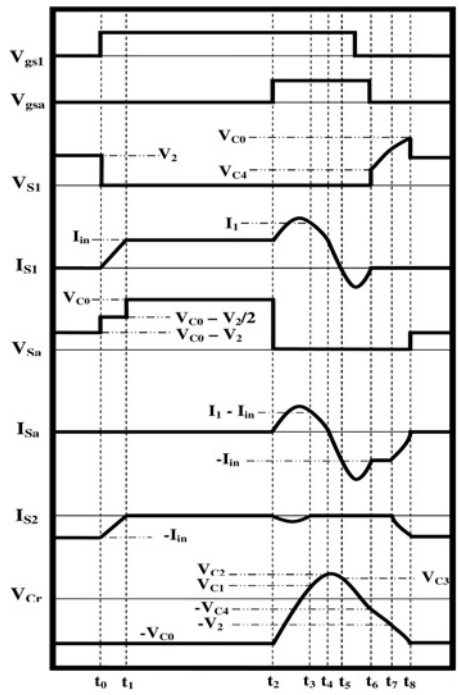

Fig. 3 *Converter theoretical waveforms in boost mode of operation*

Interval 5: $[t_4 - t_5]$ (Fig. 2*e*): The resonance between L_{S1} and C_r continues through S_1 and body diode of S_a and thus, S_a can be turned off under ZCS condition. S_1 current equation and C_r voltage are

$$I_{S1} = I_{in} - \frac{V_{C2}}{Z_1}\sin(\omega_1(t - t_4)) \tag{9}$$

$$V_{C_r} = V_{C2}\cos(\omega_1(t - t_4)) \tag{10}$$

At the end of this interval, S_1 current reaches zero, and it is assumed that C_r discharges to V_{C3}.

Interval 6: $[t_5 - t_6]$ (Fig. 2*f*): The resonance between L_{S1} and C_r continues through the body diodes of S_1 and S_a. During this interval, S_1 can be turned off under ZCS condition. S_1 current and C_r voltage equations are as follows

$$I_{S1} = I_{in} - I_{in}\cos(\omega_1(t - t_5)) - \frac{V_{C3}}{Z_1}\sin(\omega_1(t - t_5)) \tag{11}$$

$$V_{C_r} = -Z_1 I_{in}\sin(\omega_1(t - t_5)) + V_{C3}\cos(\omega_1(t - t_5)) \tag{12}$$

At the end of this interval, body diode of S_1 turns off under ZCS condition and it is assumed that C_r discharges to $-V_{C4}$.

Interval 7: $[t_6 - t_7]$ (Fig. 2*g*): The resonance of the previous interval ends at t_6, and according to (13), C_r discharges to V_2 linearly by the input current.

$$V_{C_r} = -V_{C4} - \frac{I_{in}}{C_r}(t - t_6) \tag{13}$$

Interval 8: $[t_7 - t_8]$ (Fig. 2*h*): When C_r voltage reaches V_2, the body diode of S_2 turns on under ZCS condition. This starts a resonance between C_r and L_{S2} through the body diodes of S_2

doi: 10.1049/iet-pel.2011.0098

and S_a. S_2 current and C_r voltage equations are as follows

$$I_{S2} = -I_{in} + I_{in}\cos(\omega_1(t - t_7)) \quad (14)$$

$$V_{C_r} = -(Z_1 I_{in}\sin(\omega_1(t - t_7)) + V_2) \quad (15)$$

C_r current decreases in a sinusoidal fashion, and the body diode of S_a turns off at the end of this interval. Also, C_r voltage reaches $-V_{C0}$ which is equal to $V_2 + Z_1 I_{in}$.

Interval 9: $[t_8 - t_0 + T]$ (Fig. 2*i*): This operating interval is identical to the switch-off stage of the hard switched PWM boost converter, and the input current is transferred to the V_2 through the body diode of S_2.

2.2 Buck mode of operation

In this mode, S_2 and S_a are the main and auxiliary switches, respectively. The proposed converter has nine operating intervals in this mode depicted in Fig. 4 where the arrows refer to the actual direction of currents and the voltage polarity of C_r refer to voltage polarity at the beginning of each mode. The key waveforms of the converter in buck mode are shown in Fig. 5, according to the direction of currents and the polarity of the resonant capacitor, C_r, defined in Fig. 1. Before the first interval, it is assumed that all switches are off and the output current flows through the body diode of S_1. Also, C_r voltage is $-V_{C5}$.

Interval 1: $[t_0 - t_1]$ (Fig. 4*a*): By turning S_2 on at the beginning of this interval, L_{S1}, L_{S2}, and C_r form a resonance through S_2, and the body diodes of S_1 and S_a. Owing to L_{S1} and L_{S2}, S_2 turn on is under ZCS condition. S_1 and S_2 current equations are as follows

$$I_{S1} = -I_{out} + \frac{V_2}{2L_S}(t - t_0) - \left(\frac{V_2 - 2V_{C5}}{4Z_0}\right)\sin(\omega_0(t - t_0)) \quad (16)$$

$$I_{S2} = \frac{V_2}{2L_S}(t - t_0) + \left(\frac{V_2 - 2V_{C5}}{4Z_0}\right)\sin(\omega_0(t - t_0)) \quad (17)$$

C_r voltage equation is also presented by

$$V_{C_r} = -\left(\frac{V_2}{2} + \left(V_{C5} - \frac{V_2}{2}\right)\cos(\omega_0(t - t_2))\right) \quad (18)$$

At the end of this interval, the body diode of S_1 turns off under ZCS condition. Also, it is assumed that S_2 current reaches I_1, and C_r discharges to $-V_{C6}$.

Interval 2: $[t_1 - t_2]$ (Fig. 4*b*): In this interval, C_r and L_{S2} continue to resonate, but L_{S1} does not contribute to the resonance anymore. S_a and S_2 current and C_r voltage

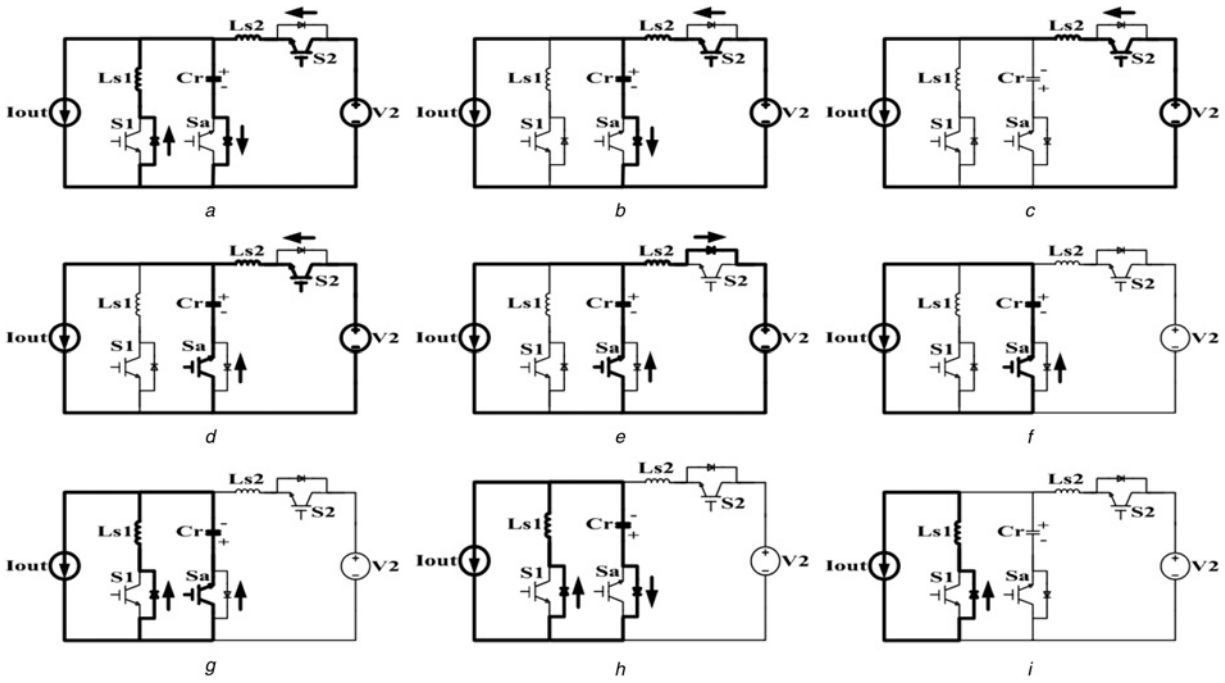

Fig. 4 *Equivalent circuit for each operating interval of the proposed converter in buck mode*

a $[t_0 - t_1]$
b $[t_1 - t_2]$
c $[t_2 - t_3]$
d $[t_3 - t_4]$
e $[t_4 - t_5]$
f $[t_5 - t_6]$
g $[t_6 - t_7]$
h $[t_7 - t_8]$
i $[t_8 - t_0 + T]$

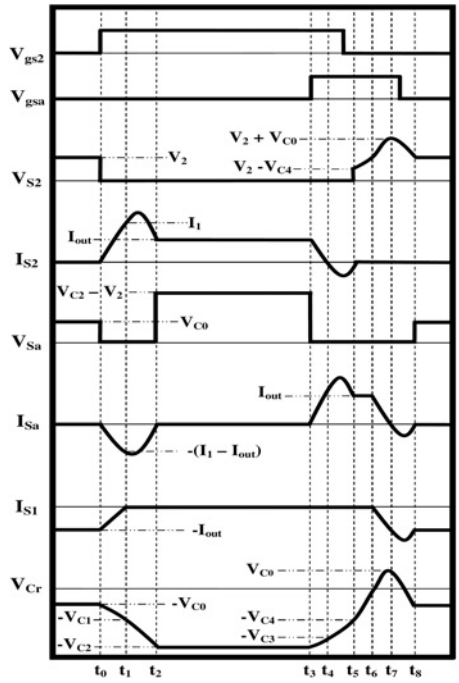

Fig. 5 *Converter theoretical waveforms in buck mode of operation*

equations are as follows

$$I_{S2} = I_{\text{out}} + (I_1 - I_{\text{out}})\cos(\omega_1(t - t_1)) + \left(\frac{V_2 - V_{C6}}{Z_1}\right) \times \sin(\omega_1(t - t_1)) \tag{19}$$

$$I_{S_a} = -(I_1 - I_{\text{out}})\cos(\omega_1(t - t_1)) - \left(\frac{V_2 - V_{C6}}{Z_1}\right) \times \sin(\omega_1(t - t_1)) \tag{20}$$

$$V_{C_r} = -(V_2 + Z_1(I_1 - I_{\text{out}})\sin(\omega_1(t - t_1)) - (V_2 - V_{C6})\cos(\omega_1(t - t_1))) \tag{21}$$

This interval ends when S_a current reaches zero in a sinusoidal fashion. Also, C_r discharges to $-V_{C7}$.

Interval 3: $[t_2 - t_3]$ (Fig. 4*c*): This operating interval is identical to the switch-on stage of the hard switched PWM buck converter. The output current flows through S_2.

Interval 4: $[t_3 - t_4]$ (Fig. 4*d*): At t_3, S_a is turned on, which results in a resonance between C_r and L_{S2} through S_2 and S_a. S_a turns on under ZCS condition, and C_r voltage reaches $-V_{C8}$. S_2 current and C_r voltage equations are presented as following

$$I_{S2} = I_{\text{out}} - \left(\frac{V_{C7} - V_2}{Z_1}\right)\sin(\omega_1(t - t_3)) \tag{22}$$

$$V_{C_r} = -(V_2 + (V_{C7} - V_2)\cos(\omega_1(t - t_3))) \tag{23}$$

This interval ends when S_2 current reaches zero.

Interval 5: $[t_4 - t_5]$ (Fig. 4*e*): The resonance between L_{S2} and C_r continues through S_a and the body diode of S_2. During this mode, S_2 can be turned off under ZCS condition. S_2 current and C_r voltage equations are presented as following

$$I_{S2} = I_{\text{out}} - I_{\text{out}}\cos(\omega_1(t - t_4)) - \left(\frac{V_{C8} - V_2}{Z_1}\right) \times \sin(\omega_1(t - t_4)) \tag{24}$$

$$V_{C_r} = -(V_2 - Z_1 I_{\text{out}}\sin(\omega_1(t - t_4)) + (V_{C8} - V_2)\cos(\omega_1(t - t_4))) \tag{25}$$

This interval ends when the body diode of S_2 turns off under ZCS condition. It is assumed that C_r voltage is $-V_{C9}$ at the end of this interval.

Interval 6: $[t_5 - t_6]$ (Fig. 4*f*): At t_5, resonance stops and the output current charges C_r linearly.

$$V_{C_r} = -V_{C9} + \frac{I_{\text{out}}}{C_r}(t - t_5) \tag{26}$$

At the end of this interval, C_r voltage reaches zero.

Interval 7: $[t_6 - t_7]$ (Fig. 4*g*): At t_6, the body diode of S_1 starts to conduct and a resonance between C_r and L_{S1} begins. S_a current and C_r voltage equations are as follows

$$I_{S_a} = I_{\text{out}}\cos(\omega_1(t - t_6)) \tag{27}$$

$$V_{C_r} = Z_1 I_{\text{out}}\sin(\omega_1(t - t_6)) \tag{28}$$

S_a current decreases in a sinusoidal fashion, and reaches zero at the end of this interval. And simultaneously C_r charges to V_{C5}.

Interval 8: $[t_7 - t_8]$ (Fig. 4*h*): The resonance between C_r and L_{S1} continues through the body diodes of S_a and S_1. During this mode, S_a can be turned off under ZCS condition. S_a current and C_r voltage equations are as following

$$I_{S_a} = -\frac{V_{C5}}{Z_1}\sin(\omega_1(t - t_7)) \tag{29}$$

$$V_{C_r} = V_{C5}\cos(\omega_1(t - t_7)) \tag{30}$$

At the end of this interval, the body diode of S_a current reaches zero and C_r voltage reaches $-V_{C5}$.

Interval 9: $[t_8 - t_0 + T]$ (Fig. 4*i*): At t_8, the body diode of S_a turns off under ZCS condition, and output current flows through the body diode of S_1. This operating interval is identical to the switch-off stage of the PWM buck converter.

3 Design considerations

The converter filter inductor and capacitor is designed like a regular PWM converter. L_{S1} and L_{S2} are the snubber inductors of main switches and should be designed like any turn on snubber [37]. Therefore C_r is designed to provide ZCS for the main switches at turn off instant. According to (9) and (22), the following equations should be satisfied in order to provide ZCS condition for the main switches

$$Z_1 < \frac{V_{C2}}{I_{\text{in}}} \tag{31}$$

$$Z_1 < \frac{V_{C7} - V_2}{I_{\text{out}}} \tag{32}$$

doi: 10.1049/iet-pel.2011.0098

In the above equations, V_{C2} and $(V_{C7} - V_2)$ are almost equal to V_2 in both boost and buck modes. Another consideration for designing C_r is the additional voltage stress of main switches in buck and boost modes. In order to limit this additional voltage stress to 20% of their voltage stress in a regular converter, the following equations should be satisfied

$$Z_1 < \frac{0.2V_2}{I_{in}} \tag{33}$$

$$Z_1 < \frac{0.2V_2}{I_{out}} \tag{34}$$

Thus, the minimum value of C_r is designed according to equations (33) and (34).

4 Experimental results

A prototype of the proposed bidirectional buck and boost converter is implemented at 50-V (low voltage) V_1 and 100-V (high voltage) V_2. The converter operates at 100 kHz and an output power of 200 W.

According to the discussions in the previous section, the designed values for L_{S1}, L_{S2} and C_r are 1.5 μH, 1.5 μH and 56 nF, respectively. Furthermore, the value of L is selected 300 μH. For all switches IRGBC20U is used. The experimental results are depicted in Figs. 6–9. Figs. 6 and 7 show the voltage and current of main and auxiliary switches in boost mode of operation, respectively. Also, Figs. 8 and 9 show the voltage and current of main and auxiliary switches in buck mode of operation, respectively. It can be observed from the figures that for all switches ZCS condition is provided at both turn-on and turn-off instants. Also in Table 1, the current peaks of the hard switching converter and the proposed soft switching converter are compared. It is important to notice that although the current peak of the main switches in the proposed soft switching converter is higher than its hard switching counterpart, the average current through the switches is the same in both converters. Since the conducting voltage of insulated-gate bipolar transistor (IGBT) is almost constant and independent of switch current, once IGBTs are used as switches; the important parameter is the average current through the switch instead of switch peak current. Also, according to the design procedure and considerations, the main switches voltage stress is only 20% higher than the hard switching counterpart.

The converter efficiency curve is shown in Fig. 10, and is compared to the regular hard switching converters, for both buck and boost modes using PSPICE software. The efficiency comparison is done with same parameters using IRGBC20U as the switches. Actually, there are not many ZCT BDCs in the literature; however, in comparison to [28] in which the main switches turn-on and the auxiliary switches turn-off are under hard switching condition, which results in higher switching losses, the proposed converter has a higher efficiency. Also, in [35], a ZCT BDC is introduced which suffers from two auxiliary switches and also because of the converter topology, the efficiency is lower than the proposed converter.

Fig. 6 *Voltage (top waveform) and current (bottom waveform) of main switch S_1 when the converter is operating in boost mode*
Vertical scale is 100 V/div or 15 A/div, and the time scale is 2.5 μs/div

Fig. 7 *Voltage (top waveform) and current (bottom waveform) of auxiliary switch S_a when the converter is operating in boost mode*
Vertical scale is 100 V/div or 12 A/div, and the time scale is 2.5 μs/div

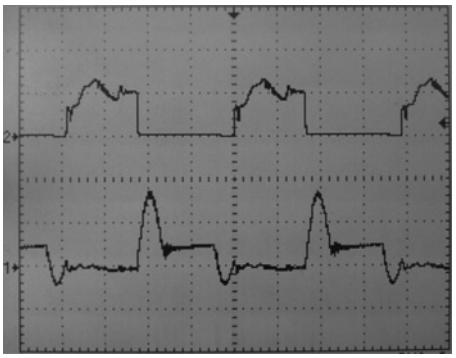

Fig. 8 *Voltage (top waveform) and current (bottom waveform) of main switch S_2 when the converter is operating in buck mode*
Vertical scale is 100 V/div or 10 A/div, and the time scale is 2.5 μs/div

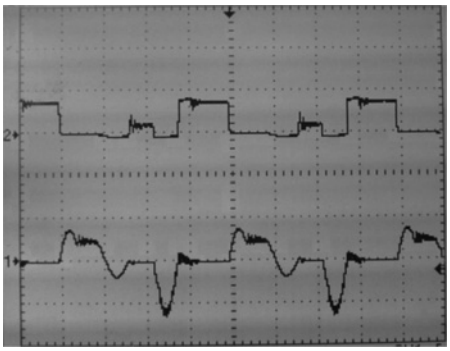

Fig. 9 *Voltage (top waveform) and current (bottom waveform) of auxiliary switch S_a when the converter is operating in buck mode*
Vertical scale is 100 V/div or 10 A/div, and the time scale is 2.5 μs/div

Table 1 Comparison of the switches current peaks in the proposed soft switching converter and the hard switching counterpart

	Main switch (S_1) current peak in boost mode	Auxiliary switch (S_a) current peak in buck mode	Main switch (S_2) current peak in buck mode	Auxiliary switch (S_a) current peak in boost mode
proposed soft switching converter	13 A	7 A	16 A	8 A
hard switching converter	6 A	–	6 A	–

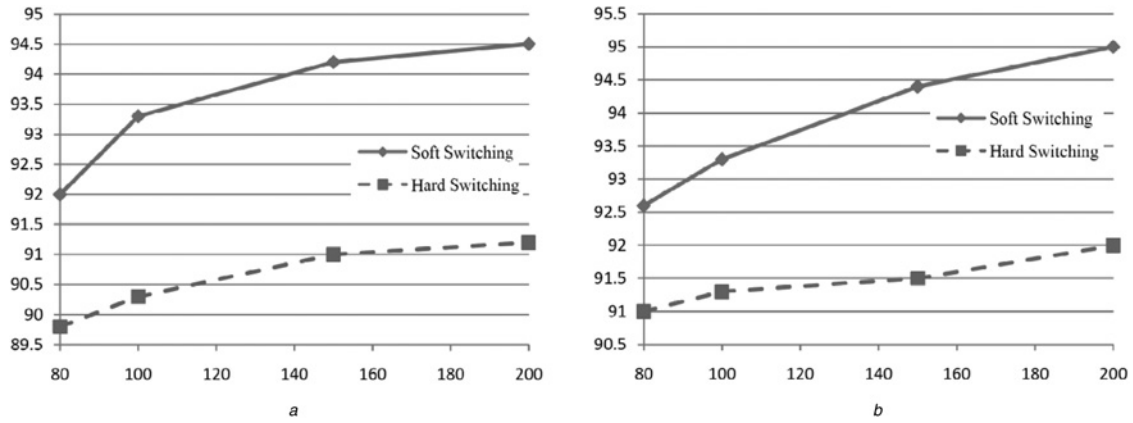

Fig. 10 *Efficiency comparison of the proposed soft switching converter (continuous line) and a hard switching buck converter (broken line) against output power*

a In boost mode
b In buck mode

5 Other ZCT bidirectional converters

Similar to the bidirectional buck and boost converter, this ZCT technique can be applied to other basic bidirectional converters to improve their efficiency, as shown in Fig. 11.

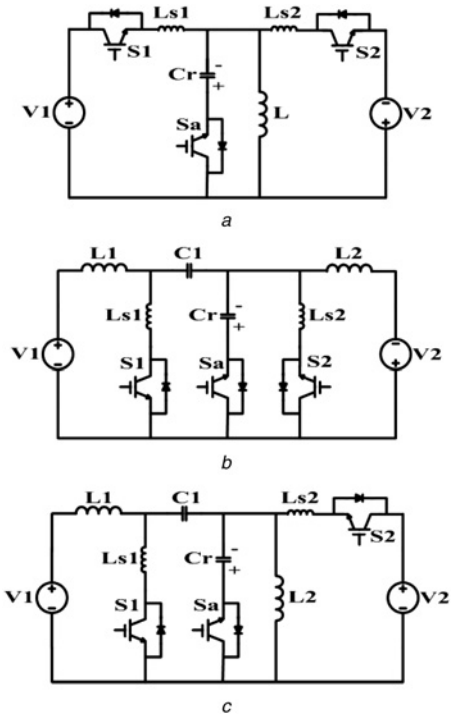

Fig. 11 *Proposed family of ZCT PWM bidirectional converters*

a Buck–boost/buck–boost
b Cuk/Cuk
c SEPIC/Zeta

In all topology variations, the theoretical operating modes are very similar to the operation of the bidirectional buck and boost converter explained in Section 2. Depending on the application, the most appropriate family member can be used. For instance, if a very smooth input and output currents are indispensable, Cuk–Cuk BDC is a proper option, as it is the only BDC with non-pulsating input and output currents.

6 Conclusion

In this paper, a new family of zero current transition bidirectional converters is introduced in which all semiconductors benefit from soft switching condition using just one auxiliary switch. The theoretical analysis for a bidirectional buck and boost converter is presented in details, and it is confirmed that ZCS is achieved for all switches. To validate the theoretical analysis, a 200 W prototype of the converter at 100 kHz is implemented. Also, the other family members of bidirectional converters are presented.

7 References

1 Tsuruta, Y., Ito, Y., Kawamura, A.: 'Snubber-assisted zero-voltage and zero-current transition bilateral buck and boost chopper for EV drive application and test evaluation at 25 kW', *IEEE Trans. Ind. Electron.*, 2009, **56**, (1), pp. 4–11
2 Amjadi, Z., Williamson, S.S.: 'Power-electronics-based solutions for plug-in hybrid electric vehicle energy storage and management systems', *IEEE Trans. Ind. Electron.*, 2010, **57**, (2), pp. 608–616
3 Marchesoni, M., Vacca, C.: 'New DC–DC converter for energy storage system interfacing in fuel cell hybrid electric vehicles', *IEEE Trans. Power Electron.*, 2007, **22**, (1), pp. 301–308
4 Camara, M.B., Gualous, H., Gustin, F., Berthon, A., Dakyo, B.: 'DC/DC converter design for supercapacitor and battery power management in

doi: 10.1049/iet-pel.2011.0098

hybrid vehicle applications—polynomial control strategy', *IEEE Trans. Ind. Electron.*, 2010, **57**, (2), pp. 587–597
5 Amjadi, Z., Williamson, S.S.: 'A novel control technique for a switched-capacitor-converter-based hybrid electric vehicle energy storage system', *IEEE Trans. Ind. Electron.*, 2010, **57**, (3), pp. 926–934
6 Nasiri, A., Nie, Z., Bekiarov, S.B., Emadi, A.: 'An on-line UPS system with power factor correction and electric isolation using BIFRED Converter', *IEEE Trans. Ind. Electron.*, 2008, **55**, (2), pp. 722–730
7 Tao, H., Duarte, J.L., Handrix, M.A.M.: 'Line-interactive UPS using a fuel cell as the primary source', *IEEE Trans. Ind. Electron.*, 2008, **55**, (8), pp. 3012–3021
8 Jang, M., Agelidis, V.: 'A minimum power-processing stage fuel cell energy system based on a boost-inverter with a bi-directional back-up battery storage', *IEEE Trans. Power Electron.*, 2011, **26**, (5), pp. 1568–1577
9 Jin, K., Yang, M., Ruan, X., Xu, M.: 'Three-level bidirectional converter for fuel-cell/battery hybrid power system', *IEEE Trans. Ind. Electron.*, 2010, **57**, (6), pp. 1976–1986
10 Schuch, L., Rech, C., Hey, H.L., Grundling, H.A., Pinheiro, H., Pinheiro, J.R.: 'Analysis and design of a new high-efficiency bidirectional integrated ZVT PWM converter for DC-bus and battery-bank interface', *IEEE Trans. Ind. Appl.*, 2006, **42**, (5), pp. 1321–1332
11 Khan, F.H., Tolbert, L.M.: 'Bi-directional power management and fault tolerant feature in a 5-kW multilevel dc-dc converter with modular architecture', *IET Power Electron.*, 2009, **2**, (5), pp. 595–604
12 Shiji, H., Harada, K., Ishihara, Y., Todaka, T., Alzamora, G.: 'A zero voltage-switching bi-directional converter for PV systems'. Proc. IEEE INTELEC, 2003, pp. 14–19
13 Gules, R., De Pellegrin Pacheco, J., Hey, H.L., Imhoff, J.: 'A maximum power point tracking system with parallel connection for pv stand-alone applications', *IEEE Trans. Ind. Electron.*, 2008, **55**, (7), pp. 2674–2683
14 Hua, G., Yang, E.X., Jiang, Y., Lee, F.C.: 'Novel zero-current-transition PWM converters', *IEEE Trans. Power Electron.*, 1994, **9**, (6), pp. 601–606
15 Meynard, T.A., Cheron, Y., Foch, H.: 'Generalization of the resonant Switch concept structures and performance'. Second European Conf. Power Electronics and Application – EPE, 1987, pp. 239–244
16 Hua, G., Leu, C.-S., Jiang, Y., Lee, F.C.Y.: 'Novel zero-voltage-transition PWM converters', *IEEE Trans. Power Electron.*, 1994, **9**, (2), pp. 213–219
17 Filho, N.P., Jose Farias, V., Carlos, L., de Freitas, L.C.: 'A novel family of DC-DC PWM converters using the self-resonance principle'. IEEE 25th Annual Power Electronics Specialists Conf., PESC' 94 Record., 20–25 June 1994, vol. 2, pp. 1385–1391
18 Bodur, H., Bakan, A.F.: 'A new ZVT-PWM DC-DC converter', *IEEE Trans. Power Electron.*, 2002, **17**, (1), pp. 40–47
19 Adib, E., Farzanehfard, H.: 'Zero-voltage-transition PWM converters with synchronous rectifier', *IEEE Trans. Power Electron.*, 2010, **25**, (1), pp. 105–110
20 Barbi, I., Bolacell, J.C.O., Martins, D.C., Libano, F.B.: 'Buck quasi-resonant converter operating at constant frequency: analysis, design, and experimentation', *IEEE Trans. Power Electron.*, 1990, **5**, (3), pp. 276–283
21 Adib, E., Farzanehfard, H.: 'Family of zero-current transition PWM converters', *IEEE Trans. Ind. Electron.*, 2008, **55**, (8), pp. 3055–3063
22 Aksoy, I., Bodur, H., Bakan, A.F.: 'A new ZVT-ZCT-PWM DC–DC converter', *IEEE Trans. Power Electron.*, 2010, **25**, (8), pp. 2093–2105
23 Dias, E.C., Freitas, L.C.G., Coelho, E.A.A., Vieira, J.B., de Freitas, L.C.: 'Novel true zero current turn-on and turn-off converter family: analysis and experimental results', *IET Power Electron.*, 2010, **3**, (1), pp. 33–42
24 Adib, E., Farzanehfard, H.: 'Family of zero current zero voltage transition PWM converters', *IET Power Electron.*, 2008, **1**, (2), pp. 214–223
25 Ivensky, G., Sidi, D., Ben-Yaakov, S.: 'A soft switcher optimized for IGBTs in PWM topologies'. Proc Tenth Annual Conf. Applied Power Electronics Conf. and Exposition, 1995. APEC 95, 5–9 March 1995, vol. 2, pp. 900–906
26 Adib, E., Farzanehfard, H.: 'Family of isolated zero-voltage transition PWM converters', *IET Power Electron.*, 2008, **1**, (1), pp. 144–153
27 Bodur, H., Bakan, A.F.: 'An improved ZCT-PWM DC-DC converter for high-power and frequency applications', *IEEE Trans. Ind. Electron.*, 2004, **51**, (1), pp. 89–95
28 Chau, K.T., Ching, T.W., Chan, C.C.: 'Bidirectional soft-switching converter-fed DC motor drives'. Proc. IEEE PESC Conf. Rec., 1998, pp. 416–422
29 Sanchis-Kilders, E., Ferreres, A., Maset, E., Ejea, J.B., Esteve, V., Jordan, J., Garrigos, A., Calvente, J.: 'Soft switching bidirectional converter for battery discharging–charging'. Proc. IEEE APEC Conf. Rec., 2006, pp. 603–609
30 Kim, I.-D., Paeng, S.-H., Ahn, J.-W., Nho, E.-C., Ko, J.-S.: 'New bidirectional ZVS PWM Sepic/Zeta DC–DC converter'. Proc. IEEE ISIE Conf. Rec., 2007, pp. 555–560
31 Lee, D.-G., Park, N.-J., Hyun, D.-S.: 'Soft-switching interleaved bidirectional DC-DC converter for advanced vehicle applications'. IEEE Power Electronics Specialists Conf., 2008, PESC 2008, 15–19 June 2008, pp. 2988–2993
32 Farzanehfard, H., Beyragh, D.S., Adib, E.: 'A bidirectional soft switched ultracapacitor interface circuit for hybrid electric vehicles', *Energy Convers. Manage.*, 2008, **49**, (12), pp. 3578–3584
33 Yan, X., Seckold, A., Patterson, D.: 'Development of a zero-voltage-transition bidirectional DC-DC converter for a brushless DC machine EV propulsion system'. 2002, IEEE 33rd Annual Power Electronics Specialists Conf., 2002. pesc 02, 2002, vol. 4, pp. 1661–1666
34 Adib, E., Farzanehfard, H.: 'Soft switching bidirectional DC-DC converter for ultracapacitor-batteries interface', *Energy Convers. Manage.*, 2009, **50**, (12), pp. 2879–2884
35 Ahmadi, M., Galvan, E., Adib, E., Farzanehfard, H.: 'New fully soft switched bi-directional converter for hybrid electric vehicles: analysis and control'. IECON 2010 – 36th Annual Conf. on IEEE Industrial Electronics Society, 7–10 November 2010, pp. 2340–2345
36 Mohammadi, M.R., Farzanehfard, H.: 'A bidirectional zero voltage transition converter with coupled inductors'. 2010 IEEE Int. Conf. on Power and Energy (PECon), 29 November–1 December 2010, pp. 57–62
37 Pressman, A.I.: 'Switching power supply design' (McGraw-Hill, New York, 1998, 2nd edn.)